Space-Air-Ground Network for Direct-to-Cell Communication

Abdullah Al Noman*†, Talip Tolga Sarı*‡, Sunday Amatare†, Gokhan Secinti‡, and Debashri Roy†
†The University of Texas at Arlington, USA, ‡ Istanbul Technical University, Turkey
Emails: {axn6368, saa3326}@mavs.uta.edu, {sarita, secinti}@itu.edu.tr, {debashri.roy}@uta.edu

***Abstract*—The growing demand for ubiquitous and resilient wireless connectivity, particularly in remote or disaster-stricken areas, highlights the limitations of traditional Direct-to-Cell (D2C) communication systems, which suffer from capacity bottlenecks, high propagation losses, and unreliable coverage. These challenges are critical barriers to achieving seamless global communication and supporting applications such as emergency response, smart infrastructure, and industrial automation, where robust connectivity directly impacts safety, operational efficiency, and societal resilience. To this end, we propose a UAV-enabled Space-Air-Ground Integrated Network (SAGIN) framework, in which UAVs operate as adaptive relays between low-earth-orbit satellites and user terminals. Our system leverages altitude-optimized UAV placement and environment-aware channel modeling, incorporating realistic ionospheric, atmospheric, multipath, and fading effects to dynamically mitigate propagation losses and optimize link reliability. We validate our approach using the NVIDIA Sionna simulator by conducting experiments across diverse environments and disaster-response scenarios. Our results demonstrate that the proposed SAGIN framework achieves a 91.7% improvement in downlink throughput compared to baseline D2C model, with a graceful degradation of 12ms end-to-end latency.**

***Index Terms*—D2C, SAGIN, UAV, D2C Communication.**

I. Introduction

Prospect of Direct-to-Cell (D2C). The increasing demand for seamless and ubiquitous connectivity, particularly in remote, under-served, and disaster-affected regions, has driven the need for D2C communication systems. D2C communication enables standard mobile phones or any user equipment to connect directly to satellites without the need for specialized hardware. This capability is revolutionizing mobile communication by extending cellular coverage far beyond the limits of terrestrial infrastructure. D2C leverages 5G and emerging 6G networks, broadcast and multicast technologies, edge AI, and massive IoT standards to provide reliable, secure, and scalable direct connectivity with mobile and IoT devices [1]. These advancements support a wide range of applications, including emergency alerting, smart infrastructure, and industrial automation. Companies such as Starlink [2], AST SpaceMobile [3], and Lynk Global [4] are at the forefront of D2C innovation.

Current Landscape of D2C. While state-of-the-art D2C communication offers powerful and flexible capabilities, significant challenges remain. These include network capacity, data rate limitations, coverage gaps, security concerns, device constraints, and operational complexity [5]. For example, AST SpaceMobile conducted 5G connectivity tests for Vodafone, AT&T, and Nokia using space-based cellular broadband, achieving download speed of up to 10 Mbps. The speed supported not only basic voice and text services but also internet browsing, file downloads, video streaming, and other applications on standard smartphones [6]. However, as communication demands continue to evolve with the advent of 6G networks and the rapid expansion of the Internet of Things (IoT), D2C technology may fall short of meeting the stringent requirements. These challenges, along with ongoing technological advancements, are driving a paradigm shift toward more sophisticated communication architectures and are stimulating active research in both academia and industry, particularly in the development of Space-Air-Ground Integrated Networks (SAGINs) [7].

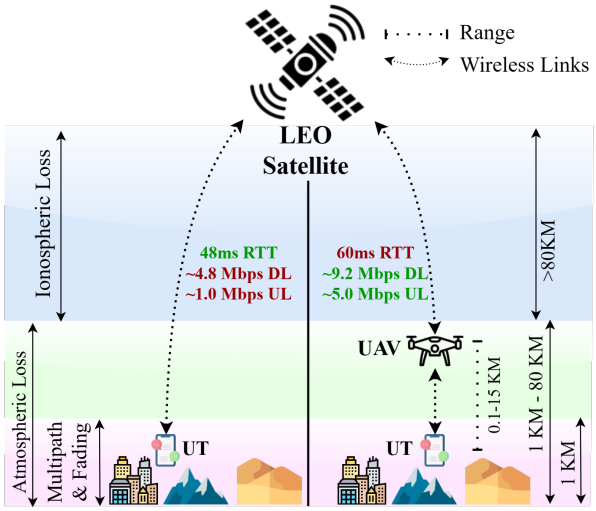

(a) Traditional D2C (b) SAGIN-enabled D2C

Fig. 1. Comparison of traditional D2C and SAGIN-enabled D2C communication. We show how communication performance can improve with UAV support, along with the effective range at each layer across various scenarios. Overall, we observe a significant increase in uplink and downlink effective throughput, while having a marginal increase in Round Trip Time (RTT). The figure is not to scale and is for illustrative purposes only.

Innovation Opportunity with SAGIN. SAGINs are emerging vertical heterogeneous network architectures that represent a promising paradigm for achieving seamless global connectivity by integrating space-based, aerial, and terrestrial commu-

*Abdullah Al Noman and Talip Tolga Sarı have equally contributed to this work.

nication infrastructures [8]. By leveraging the unique capabilities of each layer, this hierarchical and heterogeneous architecture offers enhanced flexibility, resilience, and extended coverage. This enables SAGINs to overcome traditional barriers to information sharing and support unified network operations across diverse domains. Overall, SAGINs hold significant potential for enabling multi-dimensional, ubiquitous coverage and seamless information exchange. They offer critical support for future applications such as Earth observation and mapping, Intelligent Transportation Systems (ITS), military operations, disaster response, and other mission-critical domains [9].

Proposed SAGIN-enabled D2C. Building on recent advancements in D2C communication and SAGINs, we propose a conceptual UAV-enabled SAGIN framework that leverages the Sionna channel model simulator to enable more reliable and efficient communication. Traditional D2C channel models often incorporate *ionospheric loss*, *atmospheric loss*, *multipath effects*, and *signal fading* across the entire communication link. However, ionospheric losses predominantly occur at altitudes up to 80 km, while multipath effects are primarily confined to the Earth's surface due to geographical and man-made structures. Consequently, this research introduces a UAV-based relay node within the SAGIN framework to support D2C communication. The overall D2C link is theoretically modeled as a two-hop relay communication: (a) the Low Earth Orbit (LEO) satellite to UAV link (SAT↔UAV), and (b) the UAV to User Terminal (UT) link (UAV↔UT). For realistic deployment, the SAT↔UAV link model incorporates ionospheric, atmospheric, and free-space path losses. The UAV↔UT link model considers atmospheric loss, multipath effects, and fading. The altitude-dependent characteristics of these losses, drawn from existing literature, are illustrated in Fig. 1. The proposed UAV-enabled D2C communication assumes UAV operational altitudes ranging from 100 meters to 15 km. Experimental validation, conducted in Sionna following the 3GPP TR 38.811 Non-Terrestrial Networks (NTN) standard, demonstrates that altitude-optimized UAV placement can significantly improve communication reliability and resilience.

Novel Contributions. Formally, this paper's contributions are:

C1. We propose a UAV-enabled D2C model by decoupling the uncertain channel near the ground from the more stable channel at the higher altitude. We orchestrate the theoretical formulation of D2C in terms of SAT↔UAV and UAV↔UT links which utilizes the 3GPP stochastic channel models and leverages NVIDIA's Sionna [10] simulation software.

C2. We propose a use-case-centric optimization of the UAV↦UT distance to determine the optimal UAV positioning for enhanced communication performance.

C3. We validate our framework by leveraging the 3GPP TR 38.811 standard [11], incorporating its well-established channel models as comprehensively as possible. This standard, developed from real-world measurements across diverse environments such as urban areas, mountainous regions, and deserts, provides a robust and credible foundation for simulating a wide range of communication scenarios.

C4. Experimentally we compare our UAV-enabled D2C model with a baseline D2C model without UAV support. We observe a 91.7% improvement in downlink throughput, while UAV-enabled D2C experiences an approximately 12 ms increased delay in disaster scenarios. We release our codebase for broader community use in [12].

II. Related Works and Motivation

D2C communication and SAGINs are expected to be significantly advanced through the integration of enabling technologies. These technologies aim to ensure ubiquitous coverage, accommodate heterogeneous communication scenarios, enhance network intelligence, improve spectral efficiency, and bolster security. Due *et al.* propose an open-source framework that integrates with Sionna to support the development and testing of communication systems for NTN scenarios [13]. Their work adheres to the 3GPP TR 38.811 standard and focuses on D2C communication. Sandri *et al.* present an ns-3 implementation of the 3GPP channel and antenna models for NTN scenarios [14] . They extend the ns-3 codebase with new modules to model signal attenuation in space, incorporate new mobility and fading models, and validate their accuracy through simulations against 3GPP calibration results. Cao *et al.* introduce a novel SAGIN-IoV architecture that leverages Software-Defined Networking (SDN) and Network Function Virtualization (NFV) to enhance network performance [15]. They develop an optimization framework that jointly considers energy efficiency, service latency, resource utilization, and security. Similarly, Marinho *et al.* propose a modified version of CAIN, originally designed for post-disaster 6G terrestrial networks, adapted to operate within SAGIN [16]. The new framework, SAGIN-CAIN, enables end-to-end routing from ground nodes to satellites, ensuring reliable connectivity in 3D space.

Motivation for Modeling SAGIN-enabled D2C: State-of-the-art in D2C communication offers adaptable and high-performing capabilities; however, it still faces critical challenges such as limited network capacity, data rate constraints, and coverage gaps [17]. Furthermore, traditional D2C models often assume uniform propagation losses across the entire SAT ↔ UAV link, which is an unrealistic simplification. In this paper, we propose a SAGIN-enabled D2C communication model that incorporates distinct propagation losses at the SAT ↔ UAV ↔ UT link. This more accurate and layered modeling approach aims to improve both uplink and downlink throughput compared to traditional D2C systems.

III. System Model and Problem Formulation

We design our system using stochastic channel model comprising of two hops to orchestrate the D2C communication link: (a) SAT↔UAV and (b) UAV↔UT. Both communication links are modeled by incorporating relevant propagation losses and adjusting the parameters according to the specific geographical environments. Overall, we consider three distinct geographical environments for UAV↔UT link where D2C has

stir up interest for global usage: (a) *urban (city)*, (b) *desert*, and (c) *mountain*, each characterized by unique channel conditions.

A. Communication Links

We denote the communication links for the $\texttt{UAV}\leftrightarrow\texttt{UT}$ hop of these three ground scenarios as: (a) $\text{City}_{\texttt{UAV}\leftrightarrow\texttt{UT}}$ for *city*, (b) $\text{Mountain}_{\texttt{UAV}\leftrightarrow\texttt{UT}}$ for *mountain*, and (c) $\text{Desert}_{\texttt{UAV}\leftrightarrow\texttt{UT}}$ for *desert*. However, we consider same channel model for all three scenarios for the $\texttt{SAT}\leftrightarrow\texttt{UAV}$ hop, the communication link is denoted as $\text{Upper}_{\texttt{SAT}\leftrightarrow\texttt{UAV}}$.

In the $\text{City}_{\texttt{UAV}\leftrightarrow\texttt{UT}}$ link, we consider heavy path loss, extensive shadowing, and fading with atmospheric absorption towards the higher altitude. For the $\text{Mountain}_{\texttt{UAV}\leftrightarrow\texttt{UT}}$ link, we also consider similar heavy path loss, extensive shadowing, and fading with atmospheric absorption towards the higher altitude. Where as for $\text{Desert}_{\texttt{UAV}\leftrightarrow\texttt{UT}}$ link, we consider minimal path loss, shadowing, and fading with less atmospheric absorption towards the higher altitude. In the $\text{Upper}_{\texttt{SAT}\leftrightarrow\texttt{UAV}}$ link we consider heavy ionospheric loss and atmospheric loss. We consider Doppler shifts of the LEO satellite to be compensated by the Phase Locked Loop (PLL) at the UAV receiver.

B. Channel Models

SAT↔UAV Hop. The received power $\mathcal{P}^{\texttt{RX}}_{\texttt{SAT}\leftarrow\texttt{UAV}}$ at the satellite for the $\text{Upper}_{\texttt{SAT}\leftarrow\texttt{UAV}}$ uplink is structured as:

$$\begin{aligned}\mathcal{P}^{\texttt{RX}}_{\texttt{SAT}\leftarrow\texttt{UAV}} &= \mathcal{P}^{\texttt{TX}}_{\texttt{UAV}} + \mathcal{G}_{\texttt{SAT}} + \mathcal{G}_{\texttt{UAV}} \\ &\quad - \mathcal{L}^{\texttt{FSPL}}_{\texttt{SAT}\leftarrow\texttt{UAV}} - \mathcal{L}^{\texttt{iono}}_{\texttt{SAT}\leftrightarrow\texttt{UAV}} - \mathcal{L}^{\texttt{atmos}}_{\texttt{SAT}\leftrightarrow\texttt{UAV}} - \mathcal{L}^{\texttt{sys}}_{\texttt{SAT}},\end{aligned} \tag{1}$$

where $\mathcal{P}^{\texttt{TX}}_{\texttt{UAV}}$is the transmit power of the UAV, $\mathcal{G}_{\texttt{SAT}}$ is the antenna gain of the satellite, $\mathcal{G}_{\texttt{UAV}}$ is antenna gain of the UAV, $\mathcal{L}^{\texttt{FSPL}}_{\texttt{SAT}\leftarrow\texttt{UAV}}$ is free-space path loss between UAV and satellite, $\mathcal{L}^{\texttt{iono}}_{\texttt{SAT}\leftrightarrow\texttt{UAV}}$ is ionospheric loss between satellite and UAV, $\mathcal{L}^{\texttt{atmos}}_{\texttt{SAT}\leftrightarrow\texttt{UAV}}$ is atmospheric loss between satellite and UAV, and $\mathcal{L}^{\texttt{sys}}_{\texttt{SAT}}$ is system loss at the satellite. The SNR is calculated as: $\text{SNR}_{\texttt{SAT}\leftarrow\texttt{UAV}} = \dfrac{\mathcal{P}^{\texttt{RX}}_{\texttt{SAT}\leftarrow\texttt{UAV}}}{N_{\texttt{SAT}\leftarrow\texttt{UAV}}}$, where $N_{\texttt{SAT}\leftarrow\texttt{UAV}}$ is the noise from UAV to satellite.

Similarly, the received power $\mathcal{P}^{\texttt{RX}}_{\texttt{SAT}\rightarrow\texttt{UAV}}$ at the UAV for the $\text{Upper}_{\texttt{SAT}\rightarrow\texttt{UAV}}$ downlink is formulated as:

$$\begin{aligned}\mathcal{P}^{\texttt{RX}}_{\texttt{SAT}\rightarrow\texttt{UAV}} &= \mathcal{P}^{\texttt{TX}}_{\texttt{SAT}} + \mathcal{G}_{\texttt{SAT}} + \mathcal{G}_{\texttt{UAV}} \\ &\quad - \mathcal{L}^{\texttt{FSPL}}_{\texttt{SAT}\rightarrow\texttt{UAV}} - \mathcal{L}^{\texttt{iono}}_{\texttt{SAT}\leftrightarrow\texttt{UAV}} - \mathcal{L}^{\texttt{atmos}}_{\texttt{SAT}\leftrightarrow\texttt{UAV}} - \mathcal{L}^{\texttt{sys}}_{\texttt{UAV}},\end{aligned} \tag{2}$$

where, $\mathcal{P}^{\texttt{TX}}_{\texttt{SAT}}$ is transmit power of the satellite, $\mathcal{L}^{\texttt{FSPL}}_{\texttt{SAT}\rightarrow\texttt{UAV}}$ is free-space path loss between satellite and UAV, and $\mathcal{L}^{\texttt{sys}}_{\texttt{UAV}}$ is system loss at the UAV. The SNR $\text{SNR}_{\texttt{SAT}\rightarrow\texttt{UAV}}$ is calculated by dividing the received power $\mathcal{P}^{\texttt{RX}}_{\texttt{SAT}\rightarrow\texttt{UAV}}$ and the noise $N_{\texttt{SAT}\rightarrow\texttt{UAV}}$ between satellite and UAV.

UAV↔ UT Hop. The received power $\mathcal{P}^{\texttt{RX}}_{\texttt{UAV}\leftarrow\texttt{UT}}$ at the UAV for the uplink is configured as:

$$\begin{aligned}\mathcal{P}^{\texttt{RX}}_{\texttt{UAV}\leftarrow\texttt{UT}} &= \mathcal{P}^{\texttt{TX}}_{\texttt{UT}} + \mathcal{G}_{\texttt{UAV}} + \mathcal{G}_{\texttt{UT}} \\ &\quad - \mathcal{L}^{\texttt{FSPL}}_{\texttt{UAV}\leftarrow\texttt{UT}} - \mathcal{L}^{\texttt{atmos}}_{\texttt{UAV}\leftrightarrow\texttt{UT}} \\ &\quad - \mathcal{L}^{\texttt{shadow}}_{\texttt{UAV}\leftarrow\texttt{UT}} - \mathcal{L}^{\texttt{sys}}_{\texttt{UAV}},\end{aligned} \tag{3}$$

where $\mathcal{P}^{\texttt{TX}}_{\texttt{UT}}$ is transmit power of the UT, $\mathcal{G}_{\texttt{UT}}$is antenna gain of the UT, $\mathcal{L}^{\texttt{FSPL}}_{\texttt{UAV}\leftarrow\texttt{UT}}$ is free-space path loss between UT and UAV, $\mathcal{L}^{\texttt{atmos}}_{\texttt{UAV}\leftrightarrow\texttt{UT}}$ is atmospheric loss between UT and UAV, $\mathcal{L}^{\texttt{shadow}}_{\texttt{UAV}\leftarrow\texttt{UT}}$ is shadowing loss between UT and UAV, and $\mathcal{L}^{\texttt{sys}}_{\texttt{UAV}}$ is system loss at the UAV.

For the uplinks $\text{City}_{\texttt{UAV}\leftarrow\texttt{UT}}$, $\text{Mountain}_{\texttt{UAV}\leftarrow\texttt{UT}}$, and $\text{Desert}_{\texttt{UAV}\leftarrow\texttt{UT}}$, we set different values corresponding to these parameters, details in Section IV. The SNR is calculated as: $\text{SNR}_{\texttt{UAV}\leftarrow\texttt{UT}} = \dfrac{\mathcal{P}^{\texttt{RX}}_{\texttt{UAV}\leftarrow\texttt{UT}}}{N_{\texttt{UAV}\leftarrow\texttt{UT}}}$, where $N_{\texttt{UAV}\leftarrow\texttt{UT}}$ is the noise from UT to UAV.

The received power $\mathcal{P}^{\texttt{RX}}_{\texttt{UAV}\rightarrow\texttt{UT}}$ at the $\texttt{UT}$ for downlink is configured as:

$$\begin{aligned}\mathcal{P}^{\texttt{RX}}_{\texttt{UAV}\rightarrow\texttt{UT}} &= \mathcal{P}^{\texttt{TX}}_{\texttt{UAV}} + \mathcal{G}_{\texttt{UAV}} + \mathcal{G}_{\texttt{UT}} \\ &\quad - \mathcal{L}^{\texttt{FSPL}}_{\texttt{UAV}\rightarrow\texttt{UT}} - \mathcal{L}^{\texttt{atmos}}_{\texttt{UAV}\leftrightarrow\texttt{UT}} - \mathcal{L}^{\texttt{shadow}}_{\texttt{UAV}\rightarrow\texttt{UT}}\end{aligned} \tag{4}$$

where, $\mathcal{P}^{\texttt{TX}}_{\texttt{UAV}}$ is transmit power of the UAV, $\mathcal{L}^{\texttt{FSPL}}_{\texttt{UAV}\rightarrow\texttt{UT}}$ is free-space path loss from UAV to UT, $\mathcal{L}^{\texttt{shadow}}_{\texttt{UAV}\rightarrow\texttt{UT}}$ is shadowing loss between UAV and UT. Specific parameter values defining the downlinks for the $\text{City}_{\texttt{UAV}\rightarrow\texttt{UT}}$, $\text{Mountain}_{\texttt{UAV}\rightarrow\texttt{UT}}$, and $\text{Desert}_{\texttt{UAV}\rightarrow\texttt{UT}}$ is also defined in Section IV. The SNR,$\text{SNR}_{\texttt{UAV}\rightarrow\texttt{UT}}$ is calculated by dividing the received power $\mathcal{P}^{\texttt{RX}}_{\texttt{UAV}\rightarrow\texttt{UT}}$ and the noise $N_{\texttt{UAV}\rightarrow\texttt{UT}}$ between UAV and UT.

Uplink SNR of $\texttt{SAT}\leftarrow\texttt{UAV}\leftarrow\texttt{UT}$. In our system, the UAV operate as regenerative relay to provide communication in both the downlink and uplink for $\texttt{SAT}\leftrightarrow\texttt{UAV}\leftrightarrow\texttt{UT}$ communication. Hence, the end-to-end uplink SNR $\text{SNR}_{\texttt{SAT}\leftarrow\texttt{UAV}\leftarrow\texttt{UT}}$ is set by the minimum SNR over the two hops, acting as the bottleneck created by a less potent link.

$$\text{SNR}_{\texttt{SAT}\leftarrow\texttt{UAV}\leftarrow\texttt{UT}} = \min\left(\text{SNR}_{\texttt{SAT}\leftarrow\texttt{UAV}},\, \text{SNR}_{\texttt{UAV}\leftarrow\texttt{UT}}\right) \tag{5}$$

Downlink SNR of $\texttt{SAT}\rightarrow\texttt{UAV}\rightarrow\texttt{UT}$. Similarly, the downlink SNR, $\text{SNR}_{\texttt{SAT}\rightarrow\texttt{UAV}\rightarrow\texttt{UT}}$ is calculated as:

$$\text{SNR}_{\texttt{SAT}\rightarrow\texttt{UAV}\rightarrow\texttt{UT}} = \min\left(\text{SNR}_{\texttt{SAT}\rightarrow\texttt{UAV}},\, \text{SNR}_{\texttt{UAV}\rightarrow\texttt{UT}}\right) \tag{6}$$

Modeling fading and $\mathcal{L}^{\texttt{shadow}}_{\texttt{UAV}\leftarrow\texttt{UT}}$ using Elevation-conditioned Mixture Probability. Both fading and $\mathcal{L}^{\texttt{shadow}}_{\texttt{UAV}\leftarrow\texttt{UT}}$ are modeled as elevation-conditioned random processes, with their statistical behavior varying across the three considered scenarios: (a) City, (b) Desert, and (c) Mountain. Realistically, each scenario has different level of probability for line-of-sight (LOS) and non-line-of-sight (NLOS). Hence, for each communication link, we define a '*mixture probability*' $\mathbb{P}_{\text{LOS}}(\theta, \texttt{scene})$, where $\texttt{scene} \in \{\text{City}, \text{Desert}, \text{Mountain}\}$ denote the probability that the link is in LOS and θ is the elevation angle of the UAV. In other words by integrating the mixture probability $\mathbb{P}_{\text{LOS}}$ we combine the two widely used fading models Rayleigh and Rician depending on the scene. The mixture probability $\mathbb{P}_{\text{LOS}}(\theta, \texttt{scene})$ is defined in Eq. 7 along with the scene-specific parameters in Eq. 8, where $\theta^{\texttt{scene}}_{\text{threshold}}$ is scenario specific theshold for elevation angle of UAV, $K_{\max}$ and $K_{\min} = 0$ are maximum and minimum fading values of the fading parameter, and σ_{shadow} is the shadowing coefficient.

$$\mathbb{P}_{\text{LOS}}(\theta, \texttt{scene}) = \begin{cases} 0, & \theta \leq \theta^{\texttt{scene}}_{\text{threshold}}, \\ \mathbb{P}_{\text{LOS}}(\texttt{scene}), & \theta > \theta^{\texttt{scene}}_{\text{threshold}}, \end{cases} \tag{7}$$

scene	$\theta^{\text{scene}}_{\text{threshold}}$ [°]	$\mathbb{P}_{\text{LOS}}$	$K_{\max}$	σ_{shadow}
City	30	0.10	1	10
Mountain	20	0.60	4	8
Desert	15	0.90	8	6

(8)

Overall the channel response h is generated by drawing a uniform random variable $u \sim \mathcal{U}(0,1)$:

$$h = \begin{cases} h_{\text{Rician}}(\theta), & u < P_{\text{LOS}}(\theta, \texttt{scene}), \\ h_{\text{Rayleigh}}, & \text{otherwise.} \end{cases} \tag{9}$$

Finally, the shadowing loss is formulated as a function of this mixture probability: $\mathcal{L}^{\texttt{shadow}}_{\texttt{UAV}\leftrightarrow\texttt{UT}} = f(\mathbb{P}_{\text{LOS}}(\theta, \texttt{scene}))$ for all three types of scenes. Moreover the shadowing loss $\mathcal{L}^{\texttt{shadow}}_{\texttt{UAV}\leftarrow\texttt{UT}}$ is calculated as

$$\mathcal{L}^{\texttt{shadow}}_{\texttt{UAV}\leftarrow\texttt{UT}} = \begin{cases} 0, & u < \mathbb{P}_{\text{LOS}}(\theta, \texttt{scene}), \\ \mathcal{N}(0, \sigma^2_{\text{shadow}}), & \text{otherwise.} \end{cases} \tag{10}$$

Where $\mathcal{N}(.)$ signify Normal distribution. Thus, if the elevation angle is high enough (depending on the scene), the channel will behave as a LOS channel.

C. Problem Statement

A scheme of installing UAVs as aerial relays is a flexible and agile mechanism to suppress the problems by providing better propagation conditions and shrinking the effective distance to communicate to ground users.

We formulate the problem with $N_{\texttt{UT}}$ number of UTs placed randomly over a X km $\times$ Y km region with one UAV and one satellite at $(x_{\texttt{SAT}}, y_{\texttt{SAT}}, z_{\texttt{SAT}})$. Our goal is to maximize the SNR by adjusting the UAV placement given certain placement of UTs with corresponding antenna gains. Hence, we formulate the optimization problem as 3D placement of the UAV given the locations of $N_{\texttt{UT}}$ number of UTs and their antenna gains, SAT and its antenna gain, and UAV antenna gain. Formally,

$$\begin{aligned} \max_{(x_{\texttt{UAV}}, y_{\texttt{UAV}}, z_{\texttt{UAV}})} \sum_{i=1}^{N_{\texttt{UT}}} \text{SNR}_{\texttt{SAT}\leftarrow\texttt{UAV}\leftarrow\texttt{UT}} \Big(& (x_{\texttt{SAT}}, y_{\texttt{SAT}}, z_{\texttt{SAT}}), \\ & (x_{\texttt{UAV}}, y_{\texttt{UAV}}, z_{\texttt{UAV}}), \\ & (x_{\texttt{UT}_i}, y_{\texttt{UT}_i}, z_{\texttt{UT}_i}), \\ & \mathcal{G}_{\texttt{UT}_i}, \mathcal{G}_{\texttt{SAT}}, \mathcal{G}_{\texttt{UAV}}, \\ & param(\texttt{scene}) \Big) \end{aligned}$$

subject to:

$$\begin{aligned} & 0 \le x_{\texttt{UAV}} \le X, \\ & 0 \le y_{\texttt{UAV}} \le Y, \\ & Z_{\min} \le z_{\texttt{UAV}} \le Z_{\max}. \end{aligned} \tag{11}$$

where $param(\texttt{scene})$ is retrieved from Eq. 8, the $(x_{\texttt{UAV}}, y_{\texttt{UAV}}, z_{\texttt{UAV}})$ define the optimized UAV location, Z_{min} and Z_{max} are the maximum and minimum allowable UAV altitude depending on each scene.

D. Solution

We employ Bayesian optimization for 1000 trials to solve Eq. 11, as this approach enables rapid convergence to optimal UAV placement with significantly fewer environmental probes compared to traditional grid or random search methods. The inherent sample efficiency of Bayesian optimization makes it particularly well-suited for scenarios where each evaluation is computationally expensive or time-consuming.

IV. Experiments

A. Experiment Scenario Setting

Disaster scenarios present significant challenges for wireless communication due to dynamic user distributions and harsh propagation conditions. To capture this variability, we consider a 10 km $\times$ 10 km (hence $X = 10$ and $Y = 10$) area in which 50 UTs ($N_{\texttt{UT}}$ = 50) are randomly distributed. Since users in disaster-affected regions may experience widely varying channel conditions, we assign heterogeneous antenna gains ($\mathcal{G}_{\texttt{UT}}$) of -3 dBi and 3 dBi to different UTs. Our model incorporates both downlink (SAT$\rightarrow$UAV$\rightarrow$UT) and uplink (SAT$\leftarrow$UAV$\leftarrow$UT) transmission paths. We model both of these paths fully with Sionna, following 3GPP TR 38.811 NTN standard closely. The rest of the simulation parameters can be found in Table I.

Parameter	Value	Description
f_c	2 GHz	Carrier frequency
B	1.92 MHz	System bandwidth
$z_{\texttt{SAT}}$	600 km	Satellite altitude
$z_{\texttt{UT}}$	1.5 m	User terminal (UT) altitude
$\mathcal{P}^{\text{TX}}_{\texttt{SAT}}$	40 dBm	Satellite transmit power
$\mathcal{P}^{\text{TX}}_{\texttt{UAV}}$	30 dBm	UAV transmit power
$\mathcal{G}_{\texttt{SAT}}$	30 dBi	Satellite antenna gain
$\mathcal{G}_{\texttt{UAV}}$	10 dBi	UAV antenna gain
$\mathcal{G}_{\texttt{UT}}$	(-3,3) dBi	UT antenna gain
$N_{\texttt{UT}}$	50	Number of user terminals (UTs)
$X \times Y$	$10\times$ 10 km^2	Deployment area
$\mathcal{L}^{\text{sys}}_{\texttt{UAV}}$	2 dB	System loss at UAV
$\mathcal{L}^{\text{sys}}_{\texttt{SAT}}$	2 dB	System loss at satellite
$\mathcal{L}^{\text{FSPL}}_{\texttt{SAT}\leftrightarrow\texttt{UAV}}$	$\sim$ 154 dB	FSPL between UAV and SAT
$\mathcal{L}^{\text{iono}}_{\texttt{SAT}\leftrightarrow\texttt{UAV}}$	3-5 dB	Ionospheric scintillation loss
$\mathcal{L}^{\text{atmos}}_{\texttt{SAT}\leftrightarrow\texttt{UAV}}$	$\sim$ 0.2 dB	Atmospheric loss

Table I: System parameters consistent with the channel model and problem formulation.

B. Evaluation Metrics

Our considered evaluation metrics are: (a) **SNR** to quantify the quality of the wireless links for both uplink and downlink, reflecting the impact of environmental variability and adaptive relay positioning, (b) **BLock Error Rate (BLER)** is evaluated to provide a direct measure of link reliability, especially as modulation schemes and environmental conditions change. (c) These BLER values are further utilized to estimate the expected number of retransmissions, allowing for a more realistic calculation of the **Round Trip Time (RTT)** between

user terminals and the core network. RTT is computed according to 3GPP guidelines, taking into account the scheduling, processing, and HARQ delays, as well as additional feeder-link latency. (d) Finally, we calculate the effective **throughput** by considering the total volume of successfully delivered data, normalized by retransmission counts and protocol overheads, for both uplink and downlink.

C. Competing Methods

Our comparative study is structured around three competing methods: (a) **Trad-D2C:** The baseline is traditional D2C communication, where user terminals interact directly with LEO satellites, lacking the adaptability needed for dynamic disaster environments. (b) **SAGIN-D2C:** It incorporates UAVs as regenerative relays between satellites and user terminals but without optimization of relay positioning. This architecture leverages the flexibility of aerial relays to compensate for compromised ground infrastructure, inherently improving link quality and robustness. (c) **Opt-SAGIN-D2C:** Here, both the altitude and placement of the UAVs are fine-tuned through scenario-aware algorithms, such as Bayesian optimization, to maximize SNR and overall connectivity. These three methods are evaluated under identical system parameters and environmental assumptions.

D. Results

Signal-to-Noise Ratio for Uplink and Downlink: To begin, we first look at the resulting uplink and downlink SNRs of the three methods in Figs. 2a and 2b. By having the first hop of the uplink (and last hop of the downlink) closer to the devices, we observe substantial improvements to the SNR compared to Traditional D2C. The link to the Satellite also improves due to better antenna alignment and increased antenna gain. Overall, the optimization of UAV placement brought additional improvement to SAGIN-D2C method.

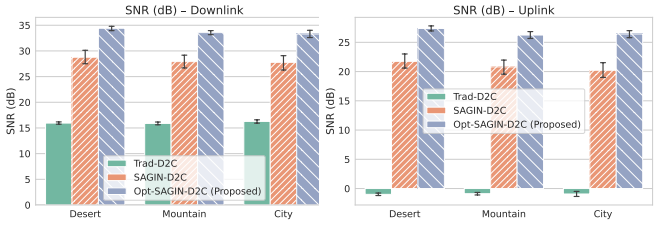

(a) Downlink SNR **(b)** Uplink SNR

Fig. 2. Comparison of downlink and uplink SNR for traditional D2C, SAGIN-D2C, and Opt-SAGIN-D2C across various environments. The closer first hop in SAGIN-based methods improves the SNR by $\sim$ 19 dB for downlink and $\sim$ 27 dB for uplink, with optimized UAV placement (Opt-SAGIN-D2C) providing the best performance.

End-to-End Latency: We measure round-trip time (RTT) from UT to core network and back in accordance with 3GPP definitions. Each transmission incurs a 0.5 ms scheduling delay, an 8 ms HARQ delay, a 3 ms processing delay, and a 5 ms feeder-link delay. To account for retransmissions, we

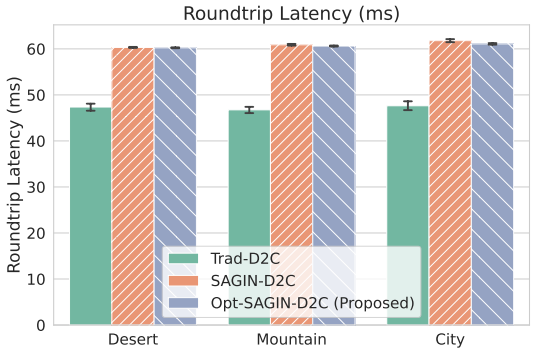

Fig. 3. End-to-end latency comparison for traditional D2C, SAGIN-D2C, and Opt-SAGIN-D2C in various environments. The results show that SAGIN causes additional delays of $\sim$ 12 ms due to usage of intermediate UAV.

compute the Estimated Transmission Count (ETX) from the BLER as

$$\text{ETX} = \frac{1}{1 - \text{BLER}} \tag{12}$$

and multiply ETX by the total per-link delay. Figure 3 presents the RTT results across urban, desert, and mountain environments. Both SAGIN and SAGIN-OPT configurations maintain approximately 60 ms latency irrespective of the scenario. In contrast, the baseline D2C approach exhibits increasing latency as channel conditions worsen, since higher BLER leads to more retransmissions.

Block Error Rates for Uplink and Downlink: We also look at the BLER for uplink and downlink to further analyze the latency results in figures 4a and 4b. We choose to use higher modulation order (256-QAM for downlink and 16-QAM for uplink) for SAGIN methods to have better throughput. As a result they have similar BLER to traditional D2C which is expected.

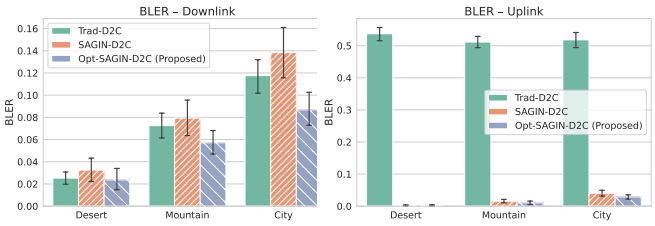

(a) Downlink BLER **(b)** Uplink BLER

Fig. 4. Comparison of downlink and uplink BLER for traditional D2C, SAGIN-D2C, and Opt-SAGIN-D2C across different environments. While closer first hop in SAGIN-based methods reduces the BLER by 33% for downlink and nearly 98% for uplink. Higher modulation order still results in elevated BLER for downlink. Optimized UAV placement (Opt-SAGIN-D2C) mitigates this effect to some extent.

Effective Throughput: We evaluate the effective throughput, defined as the successfully delivered data from user terminals (UTs) to the satellite (uplink) and from the satellite to UTs (downlink), taking retransmissions into account. As shown in

Fig. 5, both SAGIN-based methods outperform the traditional D2C baseline across all scenarios. The closer first hop to UTs in SAGIN-D2C improves the overall link quality, while the adaptive UAV positioning in Opt-SAGIN-D2C yields further gains by enhancing line-of-sight conditions. Notably, the Opt-SAGIN-D2C configuration achieves an additional 5.7% improvement in downlink throughput compared to the unoptimized SAGIN approach, highlighting the critical role of UAV placement optimization in maintaining robust performance even in challenging environments.

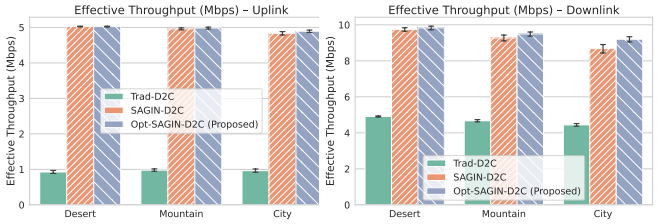

(a) Uplink throughput **(b)** Downlink throughput

Fig. 5. Effective uplink and downlink throughput comparison for D2C, SAGIN-D2C, and Opt-SAGIN-D2C in different environments. SAGIN-based methods consistently outperform the D2C baseline, with optimized UAV placement further enhancing throughput by 410% and 91.7%, for uplink and downlink respectively.

Observations: The flexibility of aerial relays in SAGIN enables dynamic adaptation to disaster scenarios, where ground infrastructure may be compromised or unavailable. By intelligently adjusting UAV altitude and horizontal placement relative to UE distributions, our framework significantly mitigates the limitations of traditional D2C communication. This results in consistently low latency and substantial throughput enhancements. Specifically, our optimized SAGIN-D2C configuration achieves a remarkable 91.7% improvement in downlink throughput compared to the baseline, with only a modest 12 ms increase in end-to-end delay. Furthermore, the uplink throughput is boosted by nearly fivefold, underscoring the potential of UAV-enabled SAGIN architectures for resilient and high-capacity disaster-response networks.

V. Conclusion

In this paper, we introduced a UAV-enabled SAGIN framework to enhance D2C communication using stochastic channel models, implemented via NVIDIA's Sionna simulator. By incorporating environment-specific propagation losses (ionospheric, atmospheric, multipath, and shadowing) and small-scale fading, we developed a two-hop decode-and-forward relay system that dynamically adapts to diverse scenarios, including urban, desert, and mountainous environments. Our optimization of UAV placement, based on Bayesian search, achieved a remarkable 91.7% improvement in downlink throughput while incurring only a modest 12 ms increase in latency. Furthermore, the uplink throughput was boosted by nearly fivefold, highlighting the critical role of UAV relay adaptability in maintaining robust performance when ground infrastructure is compromised. These results underscore the potential of UAV-enabled SAGIN architectures for resilient and high-capacity disaster-response networks. Future work will explore multi-UAV coordination and integration with emerging 6G edge intelligence to further enhance network scalability and reliability.

References

[1] K. B. Letaief, Y. Shi, J. Lu, and J. Lu, "Edge artificial intelligence for 6g: Vision, enabling technologies, and applications," *IEEE journal on selected areas in communications*, vol. 40, no. 1, pp. 5–36, 2021.

[2] Starlink, "Direct to cell," https://www.starlink.com/business/direct-to-cell, 2025, accessed: May 29, 2025.

[3] AST SpaceMobile, "Direct connection," https://ast-science.com/spacemobile-network/direct-connection/, 2025, accessed: May 29, 2025.

[4] Lynk Global, "What we do," https://lynk.world/what-we-do/, 2025, accessed: May 29, 2025.

[5] S. Chen, Y.-C. Liang, S. Sun, S. Kang, W. Cheng, and M. Peng, "Vision, requirements, and technology trend of 6g: How to tackle the challenges of system coverage, capacity, user data-rate and movement speed," *IEEE Wireless Communications*, vol. 27, no. 2, pp. 218–228, 2020.

[6] AST SpaceMobile. (2023, Sep.) Ast spacemobile achieves space-based 5g cellular broadband connectivity from everyday smartphones – another historic world first. Accessed: 2025-05-28. [Online]. Available: https://ast-science.com/2023/09/19/

[7] G. Geraci, D. López-Pérez, M. Benzaghta, and S. Chatzinotas, "Integrating terrestrial and non-terrestrial networks: 3d opportunities and challenges," *IEEE Communications Magazine*, vol. 61, no. 4, pp. 42–48, 2022.

[8] H. Cui, J. Zhang, Y. Geng, Z. Xiao, T. Sun, N. Zhang, J. Liu, Q. Wu, and X. Cao, "Space-air-ground integrated network (sagin) for 6g: Requirements, architecture and challenges," *China Communications*, vol. 19, no. 2, pp. 90–108, 2022.

[9] J. Liu, Y. Shi, Z. M. Fadlullah, and N. Kato, "Space-air-ground integrated network: A survey," *IEEE Communications Surveys & Tutorials*, vol. 20, no. 4, pp. 2714–2741, 2018.

[10] J. Hoydis, S. Cammerer, F. Ait Aoudia, A. Vem, N. Binder, G. Marcus, and A. Keller, "Sionna: An open-source library for next-generation physical layer research," *arXiv preprint*, Mar. 2022.

[11] 3rd Generation Partnership Project (3GPP), "Study on New Radio (NR) to support non-terrestrial networks," 3GPP, Technical Report TR 38.811, October 2020, https://www.3gpp.org/ftp/Specs/archive/38_series/38.811/38811-f40.zip.

[12] https://github.com/TWIST-Lab/Sionna-SAGIN.

[13] T. Düe, M. Vakilifard, C. Bockelmann, D. Wübben, and A. Dekorsy, "An open source channel emulator for non-terrestrial networks."

[14] M. Sandri, M. Pagin, M. Giordani, and M. Zorzi, "Implementation of a channel model for non-terrestrial networks in ns-3," in *Proceedings of the 2023 Workshop on ns-3*, 2023, pp. 28–34.

[15] B. Cao, J. Zhang, X. Liu, Z. Sun, W. Cao, R. M. Nowak, and Z. Lv, "Edge–cloud resource scheduling in space–air–ground-integrated networks for internet of vehicles," *IEEE Internet of Things Journal*, vol. 9, no. 8, pp. 5765–5772, 2022.

[16] R. P. Marinho, L. F. M. Vieira, M. A. M. Vieira, and A. A. F. Loureiro, "Sagin-cain: A 3d routing protocol for post-disaster sagin 6g network," in *2024 20th International Conference on Distributed Computing in Smart Systems and the Internet of Things (DCOSS-IoT)*, 2024, pp. 685–692.

[17] M. Z. Chowdhury, M. Shahjalal, S. Ahmed, and Y. M. Jang, "6g wireless communication systems: Applications, requirements, technologies, challenges, and research directions," *IEEE Open Journal of the Communications Society*, vol. 1, pp. 957–975, 2020.